Journal of Mammalian Evolution (2023) 30:363–370
https://doi.org/10.1007/s10914-023-09653-9

ORIGINAL PAPER

Growing apart: comparative cranial ontogeny in the myrmecophagous aardwolf (*Proteles cristata*) and the bone-cracking spotted hyaena (*Crocuta crocuta*)

Juliana Rajmil[1] · **Paúl M. Velazco**[2,3] · **Norberto P. Giannini**[1,2,4]

Accepted: 12 January 2023 / Published online: 17 February 2023

Abstract
Hyaenids represent an interesting case of extant low diversity but remarkable morphofunctional disparity. Hyaenas comprise three bone-cracking species, whereas the aardwolf (*Proteles cristata*) is a myrmecophagous species. Morphology of the skull and dentition reflects this functional disparity, and here we investigated postnatal ontogeny of the skull by applying multivariate allometry to 22 skull measurements taken in specimens from growth series of the spotted hyaena (*Crocuta crocuta*) and the aardwolf, which belong to hyaenid lineages that split in the middle Miocene or even earlier. We show that growth trends closely correspond to and explain the divergent morphofunctional patterning of the skull in each species. Interestingly, the smallest species —the aardwolf— showed a pronounced pattern of skull elongation, whereas in the spotted hyaena, the skull showed the strongest allometric trends in depth dimensions; these results reverse a general trend (CREA) of craniofacial elongation more pronounced in larger species, suggesting that specialization in dietary extremes can deviate developmental patterns from pervasive trends apparent in most mammalian lineages.

Keywords Bone-cracking · Dietary specialization · Hyaenidae · Myrmecophagy · Skull development

Introduction

The Hyaenidae is a group of carnivores with extant diversity reduced to only four genera and species: the spotted hyaena (*Crocuta crocuta*), the brown hyaena (*Parahyaena brunnea*), the striped hyaena (*Hyaena hyaena*) and the aardwolf (*Proteles cristata)* (Holekamp and Kolowski 2009). Hyaenids are united by a number of morphological synapomorphies but also by genetic features such as the expansion of olfactory receptor (OR) genes (Westbury et al. 2021). Genomic data indicate that extant hyaenids last shared a common ancestor at a point time estimate of 13 Ma (e.g., Westbury et al. 2021). In turn, an extensive fossil record reveals that hyaenids originated during the early Miocene in Europe and reached their diversity peak during the late Miocene, 12–6 Ma, a time dominated by dog-like hyaenas (Holekamp and Kolowski 2009). Subsequent to this large radiation, the number of species drastically decreased, and the geographic distribution of the group shrunk, nowadays being restricted to Africa and SW Asia (Werdelin and Solounias 1991). Despite their low recent diversity, hyaenas constitute a divergent group both morphologically and ecologically. Living hyaenas display ecological adaptations presently restricted to two contrasting specializations, myrmecophagy and bone-cracking hypercarnivory. Functional differences between these two morphotypes are dramatically reflected on the adult skull morphology. On one hand, the aardwolf, the sole survivor of the once diverse group of dog-like hyaenas (Protelinae), is a specialist on terrestrial social insects and particularly nasute harvester termites in the genus *Trinervitermes*, which are taken with the specialized, spatulate tongue in large quantities from aboveground, nocturnal termite foraging parties (Koehler and Richardson 1990; Skinner and Smithers 1990; Koepfli et al. 2006). The aardwolf presents widely spaced, almost

✉ Norberto P. Giannini
ngiannini@amnh.org

1 Unidad Ejecutora Lillo, CONICET-Fundación Miguel Lillo, Tucumán, Argentina

2 Department of Mammalogy, Division of Vertebrate Zoology, American Museum of Natural History, New York, NY, USA

3 Department of Biology, Arcadia University, Glenside, PA, USA

4 Facultad de Ciencias Naturales e Instituto Miguel Lillo, Universidad Nacional de Tucumán, Tucumán, Argentina

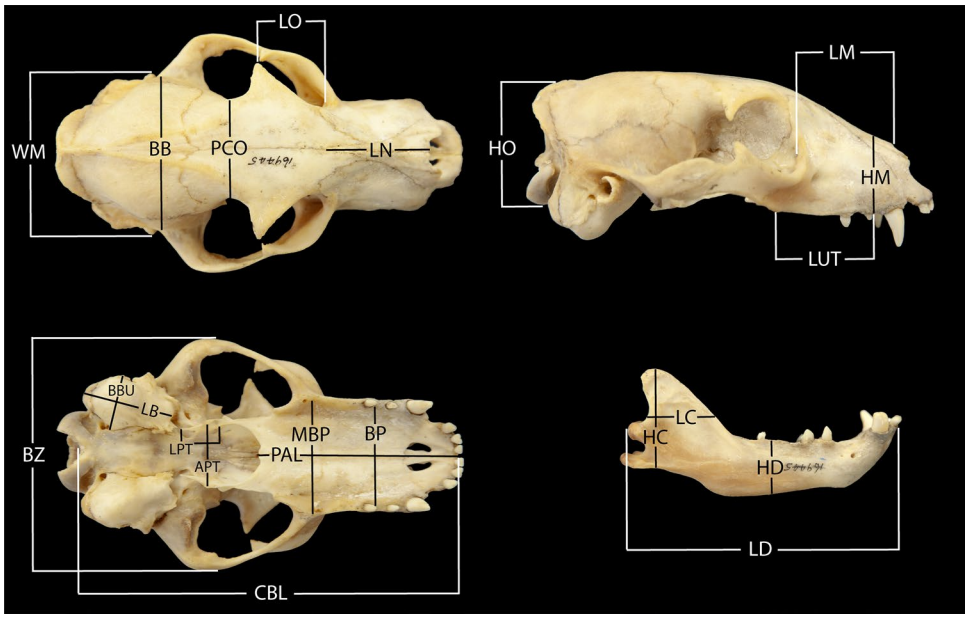

Fig. 1 Measurements taken in this study, represented in an adult skull of *Proteles cristata*. Abbreviations are listed in the text

peg-like premolars and molars; the broad, parallel-sided, slightly vaulted palate exhibits a postdental extension (Figs. 1 and 2). On the other hand, the bone-cracking hyaenids (Hyaeninae, including *Crocuta, Hyaena* and *Parahyaena*) exhibit prominent crests that provide origin to a powerful masticatory musculature, strong zygomatic arches, massive carnassials, robust skulls, and thick jaws (Fig. 3) to crush large bones scavenged from carcasses of large mammals (Koepfli et al. 2006). *Crocuta crocuta* in particular is a social hunting but also scavenging predator with extreme dietary range and plasticity, but it focuses on mid-sized (56–182 kg) ungulates (Holekamp and Kolowski 2009; Hayssen and Noonan 2021).

Thanks to its extreme diet, the spotted hyaena has been subject of extensive biomechanical and morphologic studies (Biknevicius 1996; Biknevicius and Leigh 1997; Binder and Van Valkenburgh 2000; Van Horn et al. 2003; Tanner

Fig. 2 Skulls of *Proteles cristata*: juvenile male on left (AMNH 169090) and adult female on right (AMNH 169445). Cranium in dorsal (above), ventral (middle), and lateral (below, with mandible) views. Scale bars equal 5 cm (left) and 10 cm (right)

Fig. 3 Skulls of *Crocuta crocuta*: juvenile male on left (AMNH 52058) and adult on right (AMNH 83592). Cranium in dorsal (above), ventral (middle) and lateral (below, with mandible) views. Scale bars equal 5 cm (left) and 10 cm (right)

et al. 2008, 2010; Tseng and Wang 2010). Biknevicius (1996) studied the influences of cheek teeth and the jaw in bite strength in *C. crocuta* compared with *Puma concolor* (Felidae). Another study comparing these species analyzed the development of bite force and the feeding performance in relation with dentition (Binder and Van Valkenburgh, 2000). Using finite elements, Tseng and Wang (2010) examined the functional role of the fronto-parietal sinus during biting. Tanner et al. (2010) provided a comprehensive analysis of cranial ontogeny of *C. crocuta* in a geometric morphometric framework and absolute time scale, showing that skull development in *Crocuta* is protracted; i.e., adult size and shape is achieved late in development (after sexual maturity) relative to mammalian carnivores. By contrast, there is little information on cranial ontogeny in *Proteles cristata*. Only one article described the sequence of tooth replacement in aardwolf and its fossil relatives (Gingerich 1974).

During the postnatal development of mammals, a critical change occurs from feeding on the mother´s milk to the adult diet, and more so in durophagous species such as hyaenas, which also need to eat quickly in the context of intense intra- and inter-specific interference competition (see Tanner et al. 2010). We argue that the aardwolf might also experience a significant challenge at weaning given their adult diet of noxious termites (*Trinervitermes*), tolerated only by the aardwolf among myrmecophagous mammals (see Holekamp and Kolowski 2009). The aardwolf and the spotted hyaena exhibit dramatic disparity in trophic function (see above), but still within the boundaries of dependence on a protein-rich diet. Given their phylogenetic affinities and contrasting morphology and diet, the aardwolf and the spotted hyaena are excellent candidates for comparative studies on skull development. In order to understand the extreme and divergent specializations observed in the skull of adults of these two species, we undertook a study of their postnatal ontogenetic trajectories. These species provided the opportunity to examine major morphofunctional disparity from an ontogenetic perspective within the phylogenetically controlled setting of closely related species.

Materials and methods

The species

The aardwolf (*Proteles cristata)* is the smallest among extant hyaenids (8–14 kg; Smithers 1983). It is a solitary species and a nocturnal forager that is socially monogamous (Koehler and Richardson 1990). Females give birth to 2-5 cubs after a 90-day gestation period. Cubs start feeding on termites 9-12 weeks after birth but are weaned at ca. four months of age (Koehler and Richardson 1990; Sliwa 1996).

In contrast to aardwolves, spotted hyaenas (*Crocuta crocuta*) are the largest in the family (males: 45–60 kg; females: 50–75 kg; Hofer 2002). While females tend to be larger than males, variation is large and so sexual size dimorphism can only be detected with a large sample of at least 71 specimens of each sex (McElhinny 2009). Spotted hyaenas live in clans dominated by females and are polygamous. Gestation period is 120 days; weaning is usually completed from 14–18 months of age (Frank et al. 1995; Hofer 2002).

Specimens

In this study, we analyzed cranial ontogenetic series from *Proteles cristata* (n = 28) and *Crocuta crocuta* (n = 32). The specimens examined are housed in the American Museum of Natural History (AMNH), New York; The Field Museum (FMNH), Chicago; and the United States National Museum (USNM), Smithsonian Institution, Washington DC. Specimens examined were, for *Proteles cristata*: AMNH, 146837, 87697, 169446, 169089, 34266, 187768; FMNH, 95919, 211365, 95920, 127833, 196086, 186435; USNM, 164837, 164503, 181495, 251877, 251876, 368500, 368501, 368499, 470162, 470163, 368496, 368497, 384156, 469,887, 382514, 469886; and for *Crocuta crocuta*: USNM, 162920, 161910, 162921, 162141, 163099, 162923, 162924, 350011, 162922, 161909, 163102, 163100, 163101, 163,104, 163103, 164502, 164506, 163344, 164834, 164549, 181514, 181507, 173003, 181516, 173004, 181519, 181520, 181517, 181518, 181528, 181531, 367383.

Skull variables

We measured 18 cranial and four mandibular linear variables (Fig. 1). These measurements were intended to capture overall shape and size of the skull and its most prominent structures, some of which reflect basic functional aspects; e.g., dimensions of sensory capsules as reflected in bony dimensions, and structures associated with masticatory muscles. We include the following cranial variables: skull as a whole: condylo-basal length (CBL); rostrum: length of nasals (LN), length of the muzzle (LM), height of muzzle (HM), length of palate (PAL), breadth of palate (BP), maximum breath of palate (MBP), length of pterygoid (LPT), aperture of pterygoid (APT), length of upper postcanine tooth row (LUT), maximum breadth zygomatic (BZ); neurocranium: breadth of braincase (BB), breadth of bulla (BBU), length of bulla (LB), length of orbit (LO), height of occipital plate (HO), postorbital constriction (PCO) and mastoid width (WM). For the mandible, the variables were: length of dentary (LD), height of dentary (HD), length of coronoid process (LC), and height of coronoid process (HC). Measurements were

the same for both species and were taken with a digital caliper to the nearest 0.02 mm.

Cranial allometry

We followed previous studies on cranial allometry done in other mammals (e.g., Abdala et al. 2001; Flores et al. 2003, 2006, 2010; Giannini et al. 2004, 2010; Flores and Casinos 2011; Segura and Prevosti 2012; Tarnawski et al. 2014a, b, 2015) to investigate cranial allometric trends in hyaenids from a multivariate perspective. Our ontogenetic framework is one of a continuous-growth model of mammalian development, which does not require sorting of specimens in discrete ages, such as the traditional age categories of juvenile, subadult, young adult, old-age adult; nevertheless, each age category is represented by several specimens in our samples of both species. Linear multivariate allometry is best suited for continuous-growth development; this technique is based on the generalization of the allometry equation originally proposed by Jolicoeur (1963a, b), where size is a latent variable affecting all measurements simultaneously. Following this approach, we used principal components analysis to extract the first eigenvector from a variance–covariance matrix calculated over log-transformed (base 10) data. The multivariate allometric coefficient C of a given variable p_i is represented by the corresponding element e_i of the first eigenvector rescaled to unity (i.e., $\sum e_i = 1$). The allometric trend of the variable is the statistical deviation of C from the expected isometric value V defined to be equal for all elements of e_i if all growth is isometric. V depends only on the number of variables so V = 1 / p^0.5 (Jolicoeur 1963b).

Statistical deviation from isometry was estimated using jackknife (Quenouille 1956; Tukey 1956; Manly 1997) as implemented in Giannini et al. (2004, 2010). The jackknife resampling generates pseudo-values for calculating the confidence intervals for C; if V is included in the C confidence interval, the growth pattern of the variable is isometric. To calculate the confidence interval, *n* pseudo-samples (*n* equal to the number of specimens) were generated by removing one specimen at a time. Then, the first PCA eigenvector was recalculated from the reduced matrix. For each removal cycle, a jackknife pseudo-value ê*j was obtained with the formula:

$$\hat{e} * j = n\,\hat{e} - (n-1)\hat{e} - j$$

where ê is the observed value of the corresponding C of the cranial variable X, and ê-*j* is the value of C obtained by removal of specimen *j* (Manly 1997). The jackknife estimate of C*j* = ê**j* / n. The sampling bias is C–C*j*. Pseudo-values were also used to calculate SE and then 95% and 99% confidence intervals for C. This interval may be sensitive to extreme pseudo-values, thereby failing to detect allometry; so, we trimmed the *m* largest and *m* smallest pseudo-values (here *m* = 1) and recalculated confidence intervals (see Manly 1997). Wide untrimmed confidence intervals indicate an effect of extreme pseudovalues and so trimmed intervals were chosen. These analyses were implemented in a script in the R platform (R Core Team 2020); the script is available upon request to the corresponding author.

Results and discussion

Skull allometry in the spotted hyaena

The average estimated bias in trimmed (0.0007) versus untrimmed (0.0022) analyses slightly favoured the former and so this result was selected for further interpretation. No difference in the allometric variables was observed between 95% and 99% confidence intervals, which suggests that extreme pseudovalues were not affecting the confidence interval (Online Resource 1). In this species, 31.8% of the ontogenetic growth trends were isometric and involved seven variables (LPT, HM, LN, CBL, BP, BBU, LD), while the remaining variables exhibited allometric trends (Online Resource 1). Eight variables (36.4%) were allometrically "positive" (LM, HO, PAL, LUT, BZ, LC, HC, HD) and seven variables (31.8%) were allometrically "negative" (LO, MBP, LB, APT, WM, PCO, BB).

Skull allometry in the aardwolf

The average estimated bias in both trimmed and untrimmed analyzes was essentially identical (ca. 0.002). In turn, the 95% confidence interval recovered more allometric variables; thus, for *Proteles*, we interpreted the results from the trimmed analysis with 95% confidence interval (Online Resource 1), as in *Crocuta* (see above). Four variables (18.2%) were isometric (LPT, LUT, BP, HD) in *Proteles*. Eight variables (36.4%) were allometrically "positive" (CBL, LN, LM, PAL, BZ, LD, LC, HC), and ten variables (40.9%) were allometrically "negative" (LO, HM, HO, MBP, BBU, LB, APT, WM, PCO, PCO).

Comparative skull growth and evolutionary divergence

Proteles (Fig. 2) differed from *Crocuta* (Fig. 3) in the allometric trends of nine out of 22 variables (40.9%; Online Resource 1, Fig. 4). We identified three major sets of variables that encapsulate ontogenetic differences of functional significance between these species.

The first set includes five variables that were more positively allometric in *Proteles* than in *Crocuta*, specifically

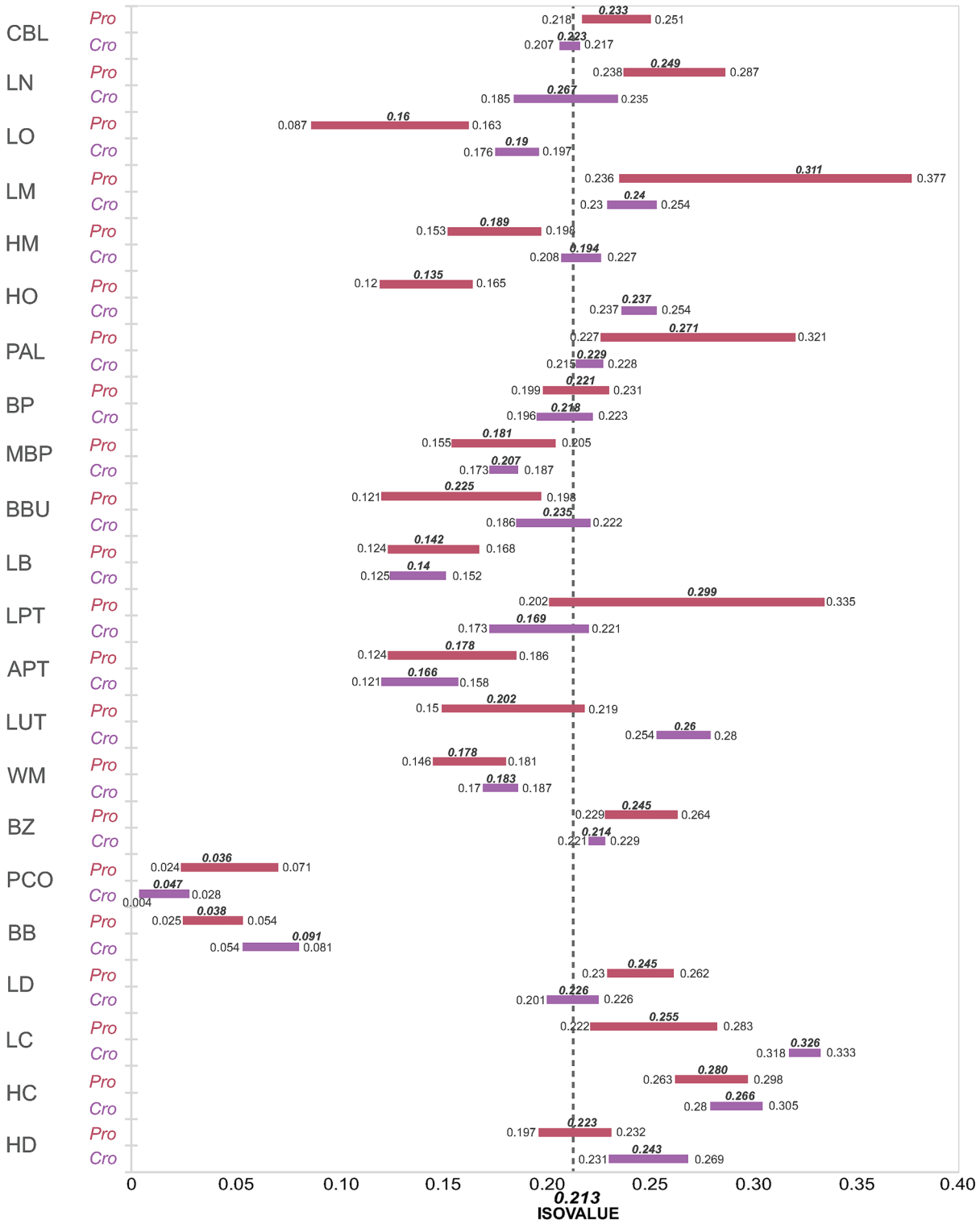

Fig. 4 Allometric trends in *Proteles cristata* (Pro) and *Crocuta crocuta* (Cro). Variables are on the vertical axis (see abbreviations in text). Variation in allometry coefficient is on the horizontal axis; expected value under isometry (0.213 for this sample; see text) is indicated with a dashed vertical line. Confidence interval (CI; 95%) is represented by a horizontal bar in each variable and species; numbers close to the bar extreme indicate lower and higher CI values under trimmed jackknife resampling, and the value above each bar is the observed coefficient of allometry for each variable and species (see Online Resource 1)

condylobasal length (CBL), and lengths of muzzle (LM), nasals (LN), palate (PAL), and dentary (LD). These are all variables that measure longitudinal dimensions of the skull (CBL) and muzzle (all others) and, in combination, their positive allometry indicate elongation of the skull in the antero-posterior axis. By contrast, for these variables *Crocuta* showed multivariate allometric coefficients that were either isometric (LD, LN, CBL), or less positively allometric than in *Proteles* (LM, PAL). A functional interpretation of these trends in *Proteles* point to the myrmecophagous habits of this species and a convergence with other mammals that specialize in feeding on social insects that also exhibit elongated skulls as compared with non-myrmecophagous relatives; these convergences extend to many other morphological aspects, such as evolutionary reduction or loss of dental pieces (e.g., anteaters, pangolins, aardvark; Redford, 1987).

Another set of variables showed strongly opposing trends in *Proteles* and *Crocuta,* which reflected a greater ontogenetic divergence in association with contrasting feeding habits; the growth pattern of all these variables were related to the relative robustness of the masticatory apparatus in *Crocuta*, as opposed to the gracile skull in *Proteles*. First, the length of the upper postcanine toothrow (LUT) was strongly positive in *Crocuta* and isometric in *Proteles* (Fig. 4). This measurement represents the size of the masticatory apparatus in antero-posterior linear dimension, and the difference between the ontogeny of the species is remarkable (cf. Figs. 2 and 3). *Proteles* exhibits a weak postcanine dentition characteristic of myrmecophagous species for which mastication is not required (ants and termites are eaten whole together with nest material and other detritus; Holekamp and Kolowski 2009). By contrast, *Crocuta* is a hypercarnivore specialized in cracking long bones of large mammals (Hayssen and Noonan 2021), for which the postcanine dentition is used. Next, the heights of muzzle (HM) and dentary (HD) growth isometricaly and allometrically positively, respectively, in *Crocuta*, reflecting the robust condition of the muzzle in the adult, whereas these variables are allometrically negative and isometric in *Proteles*, respectively (Figs. 2 and 3), reflecting the growth of a comparatively weak rostrum. The last two variables in this set were linked to the temporal muscle origin and insertion. The occipital height (HO) grew positively in *Crocuta,* resulting in a strong nuchal crest and an associated origin of the posterior temporal and nuchal muscles (Fig. 5); likewise, the length of the coronoid process (LC), which represents the insertion of the temporal muscle, is more allometrically positive in *Crocuta* than in *Proteles* (Fig. 4). The latter shows, in addition, a strong negative allometry in the occiput, which in combination indicates a weak temporal muscle action.

The third set of variables refer to differences in sensory capsules between *Proteles* and *Crocuta*. The breadth of the auditory bulla (BBU) is negatively allometric in *Proteles* and isometric in *Crocuta*; the slower rate of growth in *Proteles*

Fig. 5 Occipital views of the skulls of *Crocuta crocuta* (above) and *Proteles cristata* (below), with juvenile males on the left and adults on the right (unknown above, female below). Specimens: AMNH 52058 (upper left; scale bar equals 5 cm), AMNH 83592 (upper right; scale bar equals 10 cm), AMNH 169090 (lower left; scale bar equals 3 cm), and AMNH 169445 (lower right; scale bar equals 5 cm)

likely just cancels out an early larger size of the organ (cf. Figs. 2, 3 and 5). This is possibly also the case with the length of orbit (LO). In most mammals, the orbit, as a typical neurocranial component, grows with negative allometry (see Abdala et al. 2001), as in both *Proteles* and *Crocuta*, but the former showed a more strongly negative allometry (Fig. 4). Because the orbit is very large in adult aardwolves (Fig. 2), the species likely is born with a proportionately larger eye that subsequently grows at a slower rate as compared with the spotted hyaena. *Crocuta* is an active nocturnal predator (Hayssen and Noonan 2021), and so is the aardwolf (Koehler and Richardson 1990); however, the latter locates termites by smell and possibly audition (Koehler and Richardson 1990). In connection with this observation, *Proteles* showed a less pronounced negative allometry in the postorbital constriction (PCO) as compared with the extreme situation in *Crocuta*, which exhibited the more negatively allometric value of the entire sample (Fig. 4). While this variable has been linked with the inner space opened during ontogeny to allocate the mass of the temporal muscle (e.g., Abdala et al. 2001), which is highly developed in *Crocuta*, this region also houses the olfactory bulb (Evans 1993). We speculate that the less pronounced negative allometry in *Proteles* may reflect the growth of a larger intracranial space for the olfactory bulb and thus a greater olfaction acuity in this species.

In addition, another set of variables exhibited similar ontogenetic trends in both species, all related to

neurocranial components. These trends were negatively allometric and were comparable to those found in most mammals sampled to date (e.g., Radinsky 1981; Flores et al. 2013; Tarnawsky et al. 2014a, b, 2015). These trends probably represent a basic growth plan of therian mammals that likely exhibit different prenatal versus postnatal allometric trends in many variables (see Wilson 2011, 2014). Therefore, these trends do not differentiate *Proteles* and *Crocuta* from each other, or from other mammals (e.g., Segura et al. 2013; del Castillo et al. 2014).

Concluding remarks

The spotted hyaena and the aardwolf lineage split dates at least from the middle Miocene (ca. 15–13 Ma; Westbury et al. 2021; Galiano et al. 2022), suggesting that the diverging allometric patterns uncovered here represent long-term evolutionary pathways in this group. However, recent genetic analyses suggest that myrmecophagy in the aardwolf evolved more recently, only 4–2 Ma in its 8.9 Ma-long branch (Westbury et al. 2021). In this period, the aardwolf diverged functionally from all other large-bodied, bone-cracking (both extant and extinct) or dog-like (extinct) hyaenids; the genetic basis of such change appears in genes related to craniofacial elongation, which showed the strongest signal of positive selection in the aardwolf genome (Westbury et al. 2021).

The skull encapsulates much of the trophic functional differences between hyaenid morphotypes. We demonstrate here the ontogenetic basis of their morphofunctional disparity, with *Proteles* skull growing with greater positive allometry in muzzle and mandible length dimensions, and *Crocuta* showing allometric trends that result in deeper mandible and skull both in the muzzle region and the occiput. This pattern of growth, and the resulting skull shape in adulthood, contradict a general trend of positive craniofacial evolutionary allometry (CREA) apparent in most mammalian lineages, by which larger species tend to exhibit a proportionally longer rostrum (Cardini 2019). This suggests that specialization in dietary extremes can effectively revert the evolutionary inertia of pervasive developmental patterns.

Supplementary information The online version contains supplementary material available at https://doi.org/10.1007/s10914-023-09653-9.

Acknowledgements We thank CONICET for institutional support. We thank Bruce Patterson (The Field Museum, Chicago), Nancy Simmons and Eileen Westwig (American Museum of Natural History, New York), Don Wilson and Kristofer Helgen (United States National Museum, Smithsonian Institution, Washington DC), for granting access to specimens under their care. We acknowledge funding from a visiting scholarship award from The Field Museum to JR; PICT 2015-2389, PICT 2016-3682, and PIP 2021-23 11220200102778CO (Argentina) to NPG.

Data Availability Raw data are available from the corresponding author upon request.

References

Abdala F, Flores DA, Giannini NP (2001) Postweaning ontogeny in the skull in *Didelphis albiventris*. J Mammal 82:190-200

Biknevicius AR (1996) Functional discrimination in the masticatory apparatus of juvenile and adult cougars (*Puma concolor*) and spotted hyaenas (*Crocuta crocuta*). Can J Zool 74:1934-1942

Biknevicius AR, Leigh SR (1997) Patterns of growth of the mandibular corpus in spotted hyenas (*Crocuta crocuta*) and cougars (*Puma concolor*). Zool J Linn Soc 120:139-161

Binder WJ, Van Valkenburgh B (2000) Development of bite strength and feeding behaviour in juvenile spotted hyenas (*Crocuta crocuta*). J Zool 252:273-283

Cardini A (2019) Craniofacial allometry is a rule in evolutionary radiations of placentals. Evol Biol 46:239-248

del Castillo DL, Flores DA, Cappozzo HL (2014) Ontogenetic development and sexual dimorphism of franciscana dolphin skull: A 3D geometric morphometric approach. J Morphol 275:1366-1375

Evans HE (1993) Miller's Anatomy of the Dog. W.B. Saunders Company, Philadelphia

Flores DA, Casinos A (2011) Cranial ontogeny and sexual dimorphism in two new world monkeys: *Alouatta caraya* (Atelidae) and *Cebus apella* (Cebidae). J Morphol 272:744-757

Flores DA, Giannini NP, Abdala F (2003) Cranial ontogeny on *Lutreolina crassicaudata* (Didelphidae): a comparison with *Didelphis albiventris*. Acta Theriol 48:1-9

Flores DA, Giannini NP, Abdala F (2006) Comparative postnatal ontogeny of the skull in an australidelphian metatherian, *Dasyurus albopunctatus* (Marsupialia: Dasyuromorphia: Dasyuridae). J Morphol 267:426-440

Flores DA, Abdala F, Giannini NP (2010) Cranial ontogeny of *Caluromys philander* (Didelphidae: Caluromyinae): a qualitative and quantitative approach. J Mammal 91:539-550

Flores DA, Giannini NP, Abdala F (2013) Post-weaning cranial ontogeny in two bandicoots (Mammalia, Peramelomorphia, Peramelidae) and comparison with carnivorous marsupials. Zool 116:372-384

Frank L, Holekamp KE, Smale L (1995) Dominance, demography, and reproductive success of female spotted hyenas. In: Sinclair A, Arcese P (eds) Serengeti II: Dynamics, Management, and Conservation of an Ecosystem. University of Chicago Press, Chicago, pp 364-384

Galiano H, Tseng ZJ, Solounias N, et al (2022) A new aardwolf-line fossil hyena from Middle and Late Miocene deposits of Linxia Basin, Gansu, China. Vertebrat Palasiatic 60:81-116

Giannini NP, Abdala F, Flores DA (2004) Comparative postnatal ontogeny of the skull in *Dromiciops gliroides* (Marsupialia: Microbiotheriidae). Am Mus Novit 3460:1-17

Giannini NP, Segura V, Giannini MI, Flores D (2010) A quantitative approach to the cranial ontogeny of the puma. Mamm Biol 75:547-554

Gingerich P (1974) *Proteles cristatus* Sparrman from the Pleistocene of South Africa, with a note on tooth replacement in the aardwolf (Mammalia: Hyaenidae). Ann Transvaal Mus 29(4):49-55

Hayssen V, Noonan P (2021) *Crocuta crocuta* (Carnivora: Hyaenidae). Mamm Species 1000:1-22

Hofer H (2002) "Spotted Hyaena" (On-line). IUCN species survival commission hyaenidae specialist group. Accessed 31 Mar 2004 at http://www.hyaena.ge/spotted.htm

Holekamp KE, Kolowski JM (2009) Hyaenidae (Hyaenas). In: Wilson DE, Mittermeier RA (eds) Handbook of the Mammals of the World. Vol 1. Carnivores. Lynx Edicions, Barcelona, pp 234-260
Jolicoeur P (1963a) The multivariate generalization of the allometry equation. Biometrics 19:497-499
Jolicoeur P (1963b) The degree of generality of robustness in *Martes americana*. Growth 27:1-27
Koehler CE, Richardson PRK (1990) *Proteles cristatus*. Mamm Species 363:1-6
Koepfli K-P, Jenks SM, Eizirik E, et al (2006) Molecular systematics of the Hyaenidae: relationships of a relictual lineage resolved by a molecular supermatrix. Mol Phylogenet Evol 38:603-620
Manly BFJ (1997) Randomization, bootstrap, and Monte Carlo methods in biology. Chapman & Hall, New York
McElhinny T (2009) Morphological variation in a durophagous carnivore, the spotted hyena, *Crocuta crocuta*. Dissertation, Michigan State University, Ann Arbor.
Quenouille MH (1956) Notes on bias in estimation. Biometrika 43:353-360
R Core Team (2020) R: a language and environment for statistical computing. R Foundation for Statistical Computing, Vienna, Austria. Available at R-project.org.
Radinsky LB (1981) Evolution of skull shape in carnivores. I. Representative modern carnivores. Biol J Linn Soc 15:369-388
Redford KH (1987) Ants and termites as food. In: Genoways HH (ed) Current Mammalogy. Springer, Boston, MA, pp 349-399
Segura V, Prevosti F (2012) A quantitative approach to the cranial ontogeny of *Lycalopex culpaeus* (Carnivora: Canidae). Zoomorphology 131:79-92
Segura V, Prevosti F, Cassini G (2013) Cranial ontogeny in the Puma lineage, *Puma concolor*, *Herpailurus yagouaroundi*, and *Acinonyx jubatus* (Carnivora: Felidae): a three-dimensional geometric morphometric approach. Zool J Linn Soc 169:235-250
Skinner JD, Smithers RHN (1990) The Mammals of the Southern African Subregion, 2nd ed. University of Pretoria, Pretoria
Sliwa A (1996) A functional analysis of scent marking and mating behaviour in the aardwolf *Proteles cristatus*. Dissertation, University of Pretoria
Smithers RHN (1983) The Mammals of the Southern African Subregion. University of Pretoria, CTP Book Printers, Cape Town
Tanner JB, Dumont ER, Sakai ST, et al (2008) Of arcs and vaults: the biomechanics of bone-cracking in spotted hyenas (*Crocuta crocuta*). Biol J Linn Soc 95:246-255
Tanner JB, Zelditch ML, Lundrigan BL, Holekamp KE (2010) Ontogenetic change in skull morphology and mechanical advantage in the spotted hyena (*Crocuta crocuta*). J Morphol 271:353-365
Tarnawski BA, Cassini GH, Flores DA (2014b) Skull allometry and sexual dimorphism in the ontogeny of the southern elephant seal (*Mirounga leonina*). Can J Zool 92:19-31
Tarnawski BA, Cassini, GH, Flores DA (2014a) Allometry of the postnatal cranial ontogeny and sexual dimorphism in *Otaria byronia* (Otariidae). Acta Theriol 59:81–97
Tarnawski BA, Flores DA, Cassini GH, Cappozzo LH (2015) A comparative analysis on cranial ontogeny of South American fur seals (Otariidae: *Arctocephalus*). Zool J Linn Soc 173:249-269
Tseng ZJ, Wang X (2010) Cranial functional morphology of fossil dogs and adaptations for durophagy in *Borophagus* and *Epicyon* (Carnivora, Mammalia). J Morphol 271:1386-1398
Tukey JW (1956) Bias and confidence in not quite large samples. Ann Math Stat 23:614
Van Horn RC, McElhinny TL, Holekamp KE (2003) Age estimation and dispersal in the spotted hyena (*Crocuta crocuta*). J Mammal 84:1019-1030
Westbury MV, Le Duc D, Duchêne DA, et al (2021) Ecological specialization and evolutionary reticulation in extant Hyaenidae. Mol Biol Evol 38(9):3884-3897
Werdelin L, Solounias N (1991) The Hyaenidae: taxonomy, systematics and evolution. Foss Strata 30:1-104
Wilson LAB (2011) Comparison of prenatal and postnatal ontogeny: cranial allometry in the African striped mouse (*Rhabdomys pumilio*). J Mammal 92:407-420
Wilson LAB (2014) Cranial suture closure patterns in Sciuridae: heterochrony and modularity. J Mammal Evol 21:257-268